

# Urban traffic from the perspective of dual graph

M.-B. Hu<sup>1,2,a</sup>, R. Jiang<sup>1</sup>, Y.-H. Wu<sup>2</sup>, W.-X. Wang<sup>3</sup>, and Q.-S. Wu<sup>1</sup>

<sup>1</sup> School of Engineering Science, University of Science and Technology of China, Hefei 230026, P.R. China

<sup>2</sup> Department of Mathematics and Statistics, Curtin University of Technology, Perth WA6845, Australia

<sup>3</sup> Department of Electronic Engineering, Arizona State University, Tempe Arizona 85287-5706, USA

Received 18 February 2008 / Received in final form 22 April 2008

Published online 6 June 2008 – © EDP Sciences, Società Italiana di Fisica, Springer-Verlag 2008

**Abstract.** Urban traffic is modeled using a dual graph representation of the urban transport network, where roads are mapped to nodes and intersections are mapped to links. The proposed model considers both the navigation of the vehicles in the network and the motion of the vehicles along roads. The vehicle-holding ability of roads and the vehicle-turning ability at intersections are also incorporated. The overall handling ability of the system can be quantified by a phase transition from free flow to congestion. Simulations show that the system's handling ability greatly depends on the topology of the transportation network. In general, a well-planned grid can hold more vehicles, and its overall handling ability is much greater than that of a growing self-organized network.

**PACS.** 45.70.Vn Granular models of complex systems; traffic flow – 89.75.Hc Networks and genealogical trees – 05.70.Fh Phase transitions: general studies

## 1 Introduction

Large cities like Beijing, London, and New York are currently facing very acute traffic problem. In Beijing, almost the whole city was congested for hours after the fourth west-ring highway became jammed on Sep. 14, 2005. Similar occurrences happened again in 2006 and 2007. Traffic research has mainly focused on highway traffic [1–6] or traffic on well-planned lattice grids [7–10]. Recently, empirical evidence has shown that many transportation systems can be better described by complex networks [11,12]. The prototypes include urban road networks [13–17], nation-wide road networks [18], public transport networks [19,20], railway networks [21,22], and airline transport systems [23]. In addition, many investigations have focused on the ensuring of free traffic flow and the avoidance of traffic congestion in such transport networks [24–28].

For urban traffic, one natural approach is the “primal” representation, which considers intersections as nodes and road segments as links between the nodes. However, this representation can not characterize the common notion of “main roads” in urban traffic systems. Also, it violates the intuitive notion that an intersection is where two roads cross, not where four roads begin. Hence it cannot represent the way we describe how to navigate the road network [18], e.g., “stay on Manning Road passing 4 intersections, until you reach Kent Street and turn right.”

Here, we study urban traffic by employing a dual representation of the road network, in which a node represents a single road, and two nodes are linked if their corresponding roads intersect. This kind of transformation was first proposed in the field of urban planning and design with the name “Space Syntax” [29–31], and has been used recently to study the topological properties of urban roads [13–17]. In this dual presentation, the “main roads” of the city can be represented by the “hub nodes” in the network. The node degree is not limited and it was found that the dual degree distribution in some cities follows a power-law.

One shortcoming of the dual representation is the abandonment of metric distance. This means a street is one node no matter how long its real length is. On the other hand, the metric distance is the core element of most traffic flow studies. To avoid this problem, we propose a traffic model that considers the movement of the vehicles along the road. We show that by using some parameters that characterize the road and intersection ability, it is possible to simulate the urban traffic and determine the overall handling ability of the urban transportation system.

## 2 Dual graph of urban network and the traffic model

The basic steps of a dual representation can be illustrated as shown in Figure 1. More specifically, one should

---

<sup>a</sup> e-mail: humaobin@ustc.edu.cn

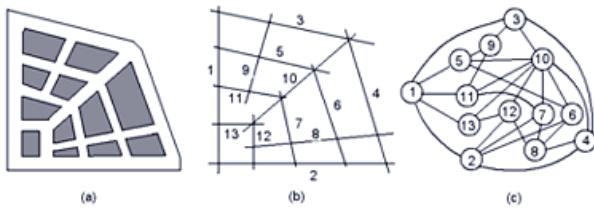


**Fig. 1.** (Color online) Sketch showing the basic steps of the dual representation. The road segments grouping method in (b) is based on the line of sight. See text for details.

first group and define the road segments (Fig. 1b). Previous studies grouped the segments either by line of sight [29–31], by their street names [13,14], or by using a threshold on the angle of incidence of segments at an intersection [15–17]. Then, in the derived “dual graph” as shown in Figure 1c, each road is turned into one node, while each intersection is turned into one link.

With this new paradigm, one can look at the urban traffic from a new perspective. From common sense, “main roads” are usually characterized by long lengths, wide road widths, many intersections, and high traffic efficiency. When main roads are congested, the entire transportation system will be in danger of a capacity drop. By contrast, the system will remain highly efficient even when some minor roads are congested. In the dual graphs, the main roads can be represented by hub nodes with many links and high efficiency. In particular, when considering traffic flow problems, the following node-related terms can be introduced:

- (1) Degree and degree distribution: the number of links connecting to the node. In the dual graph, the degree corresponds to the number of intersections along road  $i$ . The way the degree is distributed among the nodes can be investigated by calculating the degree distribution  $P(k)$ , i.e., the probability of finding nodes with  $k$  links. Networks with a power-law distribution are called scale-free networks [12].
- (2) Holding Ability  $C_i$ : the maximum number of vehicles the road can hold. This value can be calculated by:  $C_i = L_i/l_v$ , where  $L_i$  is the length of the road and  $l_v$  is the average length of the vehicles. Here we assume that the length of each road segment are the same. Thus,  $C_i$  is proportional to the degree of the node:  $C_i = \alpha \times k_i$ , where  $\alpha$  denotes the maximum number of vehicles that one road segment can hold. The system’s total holding ability is the sum of the holding ability of all nodes, that is  $C_t = \sum_i C_i$ .
- (3) Turning Ability  $T_i$ : the maximum number of vehicles turning from the road into the neighboring roads per time step. This value reflects the ability of the intersections along the road, and can also be measured in practice. In the dual graph,  $T_i$  is the maximum number of vehicles a node can send to its neighboring nodes per time step. Without losing generality, we assume that all intersections can handle the same number of vehicle-turning. Thus  $T_i$  is also proportional to the de-

gree of the node:  $T = \beta \times k_i$ , where  $\beta$  denotes the ability of one intersection.

In dual networks, the trajectory of a vehicle can be interpreted as traveling along some roads (nodes) for some distance, and then jumping from a node to another node through a link representing an intersection. In this paper, the vehicle motion along a given road is modeled in a similar way to the traffic flow on highways [1–3], and the jumping of vehicles from node to node is modeled as in the Internet traffic models [32–36]. On the base of an underlying dual infrastructure, the system evolves in parallel according to the following rules:

1. Adding Vehicles – At each step, vehicles are added to the system at a given rate  $R$ , at randomly selected nodes, and each new vehicle is given a random destination.
2. Navigating Vehicles – If a vehicle’s destination is found in its nearest neighborhood, its direction will be set to the target. Otherwise, its direction will be set to a neighbor  $n$  with probability:  $P_n = \frac{k_n^\phi}{\sum_i k_i^\phi}$ , where the sum runs over all neighbors, and  $\phi$  is an adjustable parameter reflecting the driver’s preference with the roads. It is assumed that the drivers are unaware of the entire network topology, and use a local routing strategy to find the next route. They are more ready to go to a neighboring “main road” when  $\phi > 0$ , and they are more likely to go to a minor road when  $\phi < 0$ . Generally, this assumption is acceptable in a conceptual physical model. Once a vehicle reaches its destination, it is removed from the system.
3. Motion of Vehicles along Roads – The intersections along a road  $i$  are numbered with serial integers from 1 to  $k_i$ . We use these integers to reflect the sequence of intersections along the road. When a vehicle enters a road at the  $m$ th intersection and leaves at the  $n$ th intersection, it has to travel the distance of  $d = l_0 \times |m - n|$  along the road, where  $l_0$  denotes the length of one road segment, and  $|\dots|$  denotes taking the absolute value. For the velocity, we assumed that the traffic flow is homogeneous along one given road. The mean velocity of the vehicles (the distance traveled per time step on the road) is calculated using the following equation:  $v_i = V_{max} \times (1.0 - \rho_i)$ , where  $V_{max}$  is the maximum velocity in the urban system, and  $\rho_i = N_i/C_i$  is the local vehicle density on the road ( $N_i$  is the number of vehicles on road  $i$ ). This equation reflects that the vehicles will take  $V_{max}$  when there are no vehicles on the road, and that the velocity decreases linearly until no vehicle can move when  $\rho = 1.0$ . In each time step, each vehicle on the road moves a distance  $v_i$  towards its preferred exiting intersection until  $d = 0$ , i.e., until it reaches the intersection.
4. Vehicle-Turning at Intersections – At each step, only  $T_i$  vehicles, at most, can be sent from a node to its neighboring nodes. When the number of vehicles at a selected node reaches the holding ability  $C_i$ , the node will not accept any more vehicles, and the new incoming vehicles will wait for the next opportunity.

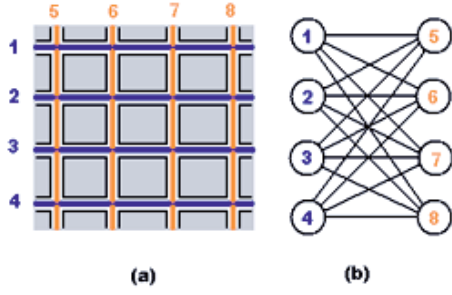


**Fig. 2.** (Color online) An example of a well-planned lattice grid: (a) the original road map; (b) the dual representation.

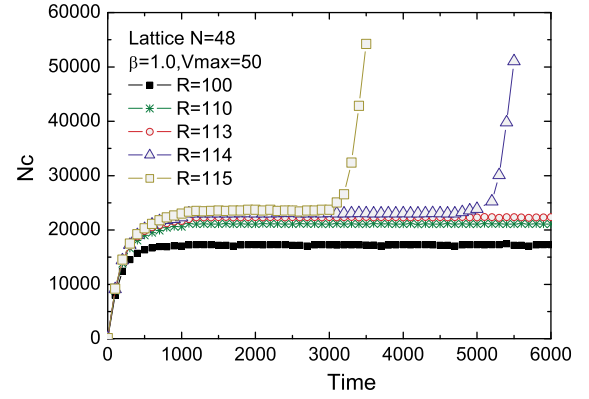
One can see that the core parameters are  $\alpha$ ,  $\beta$ , and  $V_{max}$ . Parameter  $\phi$  characterizes the behavior of drivers. Without losing generality, the road segment length  $l_0$  is assumed to be 500 meters, and the average vehicle length  $l_v$  is 10 m. Thus, we set  $\alpha = 50$ , i.e., each road segment can hold at most 50 vehicles. The parameter  $\beta$  is also set to a constant for all intersections, implying that the vehicle-turning ability for every intersection is the same. Each time step  $\delta t$  is assumed to represent 5 s in reality. Thus, if the maximum velocity is 20 m/s, the maximum possible distance a vehicle travels on the road in one step will be  $V_{max} = 100$ .

### 3 Simulation on a well-planned grid

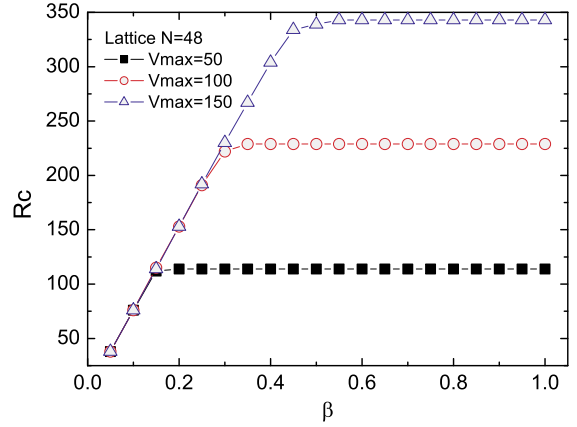
We first simulate the traffic on a well-planned grid urban network. The network consists of 24 north-south roads intersecting 24 east-west roads. An example of the original lattice grid and the dual graph of 8 roads are shown in Figure 2. The studied system can be represented by a dual graph with 48 nodes, each with the same connectivity  $k = 24$ . Thus there are no topological “main roads” in this system. For this case,  $\phi = 0$  is applied for all vehicles. Figure 3 displays the typical evolution of  $N_c(t)$ , the number of vehicles within the system. One can see that when  $R < R_c$ ,  $N_c$  increases first and then comes to saturation, indicating a balance of the number of vehicles entering the system and the number of vehicles reaching their destinations. However, when  $R > R_c$ ,  $N_c$  will suddenly increase and quickly reach the system’s total holding ability. Thus the system is congested and the vehicles accumulate in the system. Therefore, the critical  $R_c$  characterizes the phase transition from free flow to congestion and can be used to measure the system’s overall handling ability.

Figure 4 shows the variance of  $R_c$  with  $\beta$ .  $R_c$  first increases linearly with  $\beta$  and then comes to saturation. The saturated value of  $R_c$  increases with  $V_{max}$ . Thus, we can improve the overall efficiency only to some degree by enhancing the intersection efficiency. To further improve the efficiency, we should also enhance the road condition so that the vehicles can move faster on the road.

In Figure 5, one can see that  $R_c$  increases with  $V_{max}$  until a saturation is reached. Thus, as the vehicle speed can not go beyond a certain value in cities, there will be



**Fig. 3.** (Color online) Typical evolution of vehicle numbers in the grid system. The critical generating rate of vehicles is  $R_c = 113$ .



**Fig. 4.** (Color online)  $R_c$  vs.  $\beta$  with different values of  $V_{max}$ . The data are obtained by averaging  $R_c$  with ten simulations.

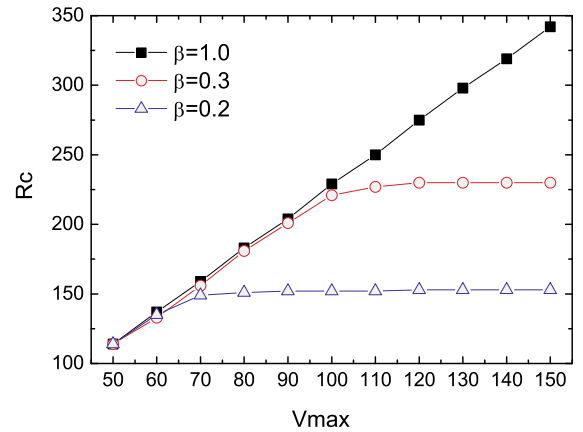


**Fig. 5.** (Color online)  $R_c$  vs.  $V_{max}$  with different values of  $\beta$ . The data are obtained by averaging  $R_c$  with ten simulations.

an unavoidable limit to the improvement of urban traffic efficiency. There is an efficiency limit simply by enhancing the intersection capacity, given that the network topology is fixed. One should think of other ways to improve urban traffic efficiency, such as adding shortcuts, developing subways, employing better navigation systems, and so on.

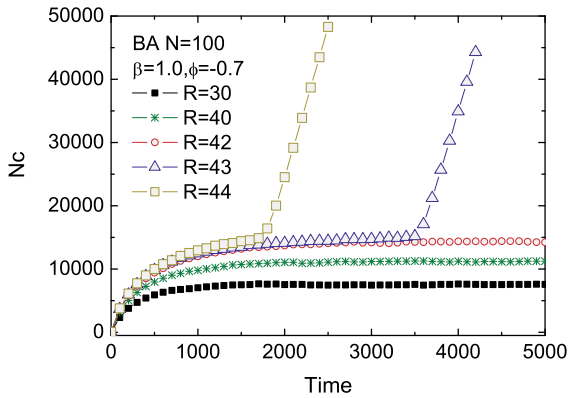


**Fig. 6.** (Color online) Typical evolution of vehicle number in the scale-free system. The critical generating rate of vehicles is  $R_c = 42$ .

#### 4 Simulation on a self-organized scale-free network

Many recent studies using dual graphs of urban systems [14–19] show that the degree distribution of most planned cities is exponential, while it follows a power-law scaling in self-organized cities. In this section, we simulate the urban traffic on a dual graph of a scale-free network. To generate the underlying infrastructure, we adopt the well-known Barabási-Albert scale-free network model [12], in which the power-law distribution of degree is in good accordance with many real observations. In this model, starting from  $m_0$  nodes fully connected by links, the system is driven by two mechanisms: (1) growth: one node with  $m$  links ( $m \leq m_0$ ) is added to the system at each step; (2) preferential attachment: the probability  $\Pi_i$  of being connected to the existing node  $i$  is proportional to the degree  $k_i$  of the node:  $\Pi_i = \frac{k_i}{\sum_j k_j}$ , where  $j$  runs over all existing nodes.

Note that we realize that the BA network model does not exactly describe a self-organized system of urban roads. We adopt this model to reflect the fact that new roads are usually built to intersect existing main roads. For example, the existing roads are often extended to new fields and branch roads are built from the extension of these roads. This mechanism can lead to the emergence of “main roads” in an urban system, and it is quite similar to the “growth” and “preferential attachment” in the BA model.

Here, we simulate the traffic on a network of  $N = 100$  nodes (roads) with  $m_0 = m = 5$ . This relatively small system can be seen as simulating the backbone of a city’s urban network. Figure 6 shows the typical evolution of vehicle numbers in the system. The same behavior as in the lattice case can be observed. Figure 7 depicts the variation of  $R_c$  with  $\phi$ . It is shown that  $R_c$  is optimized at some typical value of  $\phi_c$ . For the case of  $V_{max} = 100$ , when  $\beta > 1.0$ , the system’s overall handling ability is optimized with the maximum  $R_c \approx 42$  when  $\phi_c = -0.7$ . When  $\beta$  decreases to values below one, the system’s efficiency decreases rapidly. In addition, the optimal value of  $\phi$  increases with the de-

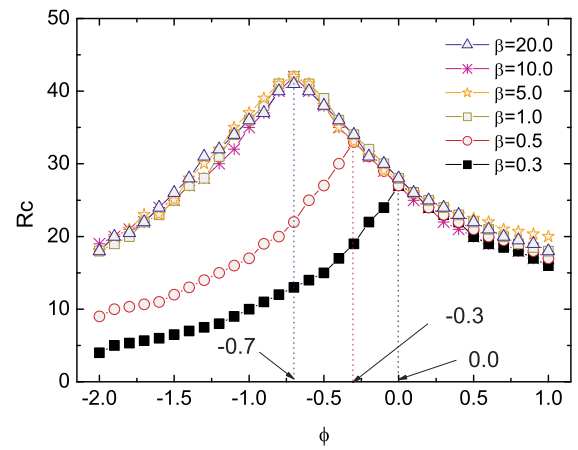


**Fig. 7.** (Color online) The system’s handling ability vs.  $\phi$  with  $V_{max} = 100$ . The data are obtained by averaging  $R_c$  over ten network realizations.

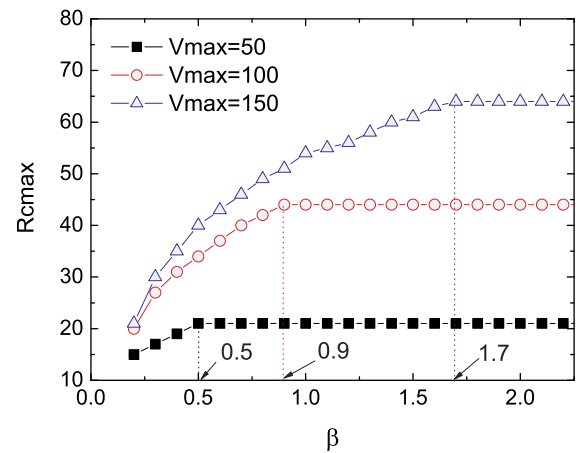
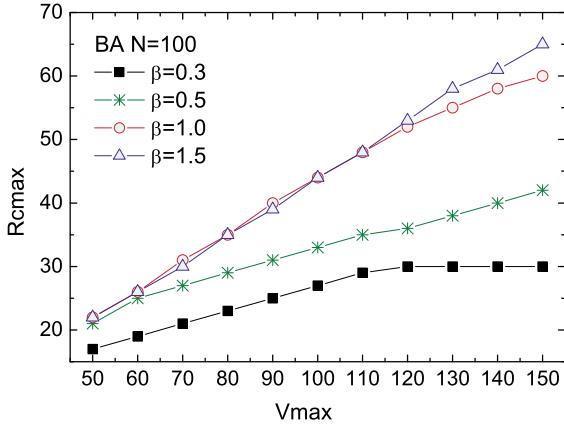


**Fig. 8.** (Color online) The system’s maximal handling ability  $R_{cmax}$  vs.  $\beta$  with different  $V_{max}$ .

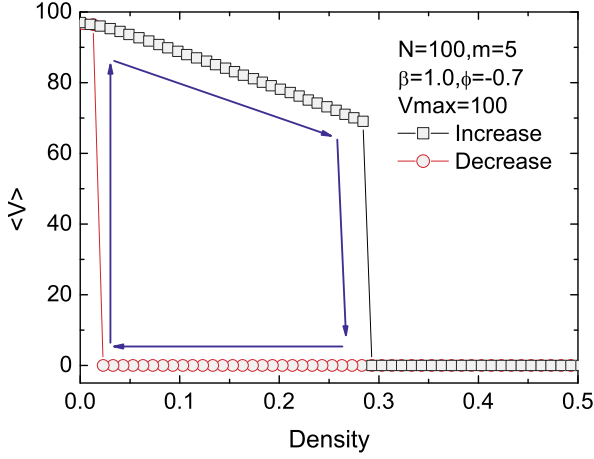
crease of  $\beta$ . When  $\beta = 0.3$ ,  $\phi_c = 0.0$ , which implies that the best strategy is a random-walk. We note that  $\phi_c < 0$  means to navigate to the minor roads first. Therefore, if the intersection turning ability and road condition are the same for both the main roads and minor roads, the best strategy for the whole system is to encourage drivers to use minor roads first.

Figure 8 shows the variation of the maximum value of  $R_c$  (the peak value in Fig. 7) with the increment of  $\beta$  for different values of  $V_{max}$ . One can see that  $R_{cmax}$  first increases and then comes to saturation. In Figure 9, the variation of  $R_{cmax}$  with  $V_{max}$  is shown. The profiles are similar to those found in the lattice grid.

Finally, we try to reproduce the dependencies of average velocity and traffic flux on vehicle density. These are important for evaluating the transit ability of a traffic system. To simulate the case where there is a constant vehicle density, the number of arrived vehicles at each time step is recorded, and the same number of vehicles are added to the system at the beginning of the next step. In Figure 10,



**Fig. 9.** (Color online) The system's maximal handling ability  $R_{cmax}$  vs.  $V_{max}$  with different  $\beta$ .



**Fig. 10.** (Color online) Average velocity vs. density. The density values corresponding to the sudden transitions are 0.29 and 0.04 respectively. The arrows show the hysteresis as a guide for the eyes.

the velocity-density relationship is displayed. Here, the vehicle density of the system is calculated by  $\rho = N_c/C_t$ . One can see that at the density of 0.29, the velocity suddenly drops to zero, indicating that the system enters into a jam state. This behavior is similar to the BML model [7], where a first order phase transition happens when the system size increases. Moreover, two branches of the fundamental diagram coexist between 0.04 and 0.29. The upper branch is calculated by adding vehicles to the system (increase density), while the lower branch is calculated by randomly removing vehicles from a jam state and allowing the system to relax after the intervention (reduce density). In this way, a hysteresis loop can be traced. In the lower branch, the velocity remains at zero until the density is very low. This is because some main roads are congested. Thus, the vehicles cannot move on these roads, and this state will not be alleviated by removing vehicles randomly from the system.

Two kinds of traffic flux are studied: the local flux and the arriving flux. The local flux is calculated as the prod-

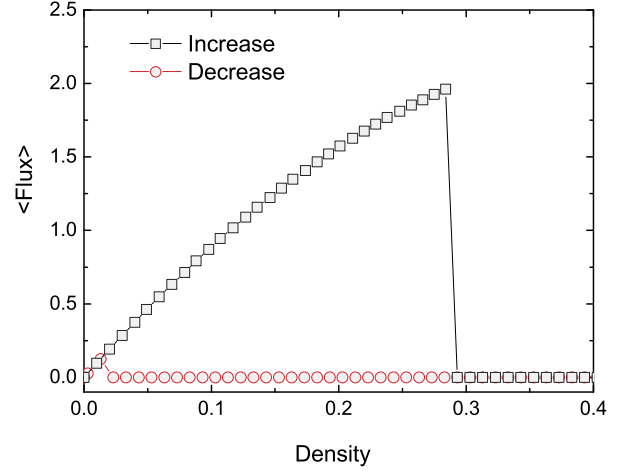


**Fig. 11.** (Color online) Flux vs. density.

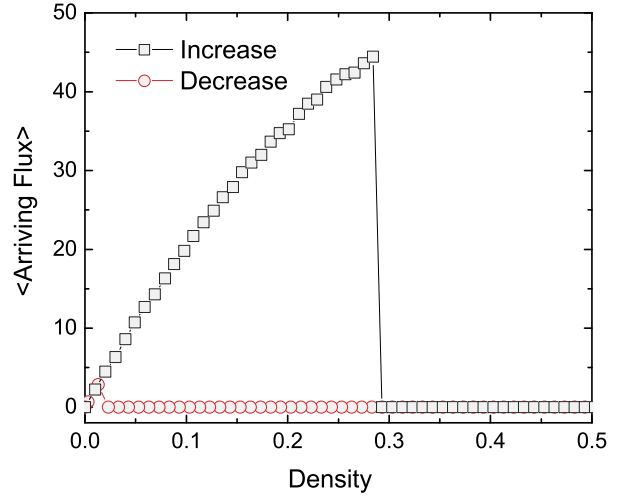


**Fig. 12.** (Color online) Arriving flux vs. density.

uct of the average velocity and vehicle density. It corresponds to the average number of vehicles passing a given spot in the system per time step. Figure 11 shows this flux-density relationship. The arriving flux is calculated as the number of vehicles that successfully reach their destination in each step. In Figure 12, the relationship between the arriving flux and the traffic density is shown. In both cases, the hysteresis exists between the same values of density as in Figure 10. Also, the maximum arriving flux (44 vehicles per step) corresponds to  $R_c = 44$  when  $V_{max} = 100$  and  $\beta = 1.0$  in Figure 8. The system's sudden drop to the jam state indicates a first-order phase transition. It can be explained as follows. According to the evolution rules, when a road is full of vehicles, the velocity will be zero and the vehicles on neighboring nodes cannot turn into it. So, the vehicles may also accumulate on the neighboring nodes, causing them to become congested. This mechanism can trigger an avalanche across the system when the density is high. Thus, a sudden phase transition happens at this point. As for the lower branch,

starting from an initial congested configuration, the system will have some congested roads that are very difficult to dissipate. These roads will reduce the system efficiency by affecting the surrounding roads until all roads are not congested. Thus, we get the lower branch.

## 5 Conclusions and discussions

In summary, urban traffic is simulated using a dual approach. The proposed model considers both the routing and motion of the vehicles. The motion along a given road is modeled in a similar way to the traffic flow on highways, and the routing of vehicles is modeled as in the Internet traffic models. The road and intersection capacities are naturally incorporated in the model. In a systemic view of overall efficiency, the model reproduces several characteristics of traffic systems, such as the phase transition from free flow to jam, hysteresis, and the velocity-density and flux-density relationships.

The phase transition from free flow to jam is similar to the change from free flow to congestion on highways [1,2], the change from free flow to synchronized flow [3], and some empirical data from highway traffic [4–6,8–10]. The dependencies of average velocity and traffic flux on vehicle density are similar to the “fundamental diagram” of highway traffic. Nevertheless, since it is difficult to obtain the relationship between overall traffic flux and overall density in urban areas, presently, we could not compare the simulation results with empirical data. In the present model, the velocity-density relationship shows a sudden drop when the density is high, which is similar to the result of the BML model [7–10].

By comparing the simulation results on a well-planned grid and on a self-organized scale-free network, our results show that the grid networks are more efficient than a self-organized one. Given that their total holding abilities ( $C_t \approx 57\,600$  and  $50\,000$ ) are almost the same, the maximum number of vehicles running on the grid is much higher than that on the scale-free network (Figs. 3 and 6), and the overall handling ability  $R_c$  has much larger value on the lattice grid (Figs. 4 and 8). This is in agreement with the previous studies which showed that homogeneous networks can bear more traffic [28,34,37]. For the navigation effect, the results show that the system will be more efficient by avoiding the central nodes, which is in agreement with a previous report [36].

The present model does not consider the roles of traffic lights, traffic signs, and other traffic control methods. So, it basically models an uncontrolled urban traffic system. Thus, the sharp drops in Figure 10 are not usually observed in real urban traffic. In our future work, the traffic control methods will be considered, together with more rational driving behaviors of the vehicles. Nevertheless, this model reproduces the nontrivial phase transition from free flow to jam, and the hysteresis. This study may be useful for evaluating the overall efficiency of urban traffic systems, and the results may also help to alleviate the congestion of modern cities and some other transportation systems. This model may also shed some light on traffic

flow controlling and the design of modern communication systems.

In future work, one can modify the model to capture more details in real traffic, such as the role of traffic control methods, and the differences between major and minor roads. Better navigation strategies can be coined in the dual perspective. The resilience of traffic systems against road failures will be of great importance and research interest.

Recently, Duch and Arenas combined a queuing theory with a random walk process on complex networks to investigate the traffic dynamics of data packets [38]. This combination is very impressive and sheds a new light on the modeling of not only information traffic, but also urban vehicle traffic, if a dual graph is considered, as was in the present paper. In our model, to effectively model the vehicle movements in urban transportation networks, we use a dual graph representation and considerably simplify the traffic dynamics of a single road by considering exclusively the correlation between vehicle density and velocity. In fact, the traffic dynamics of a single road and the interaction between roads may be better modeled by the incorporation of the queuing theory proposed in reference [38]. Queuing behavior is a common property of both information traffic on communication networks and vehicle traffic. Similar to the movement of data packets, vehicle movement on a road will be restricted by the generation of queues, which can be well described by the queuing theory. With this in mind, the present model for urban vehicle dynamics may be considerably improved by coupling the queuing theory with the dual representation. This coupling might better mimic the dynamics of vehicle traffic in urban transportation network by neglecting the microscopic dynamics of the vehicles. This investigation will be carried out in our future work. Nevertheless, the present model can characterize the dynamics of urban traffic to a certain extent by the dual representation. Moreover, the simplified vehicle dynamics of single road can significantly reduce the simulation time compared to when the microscopic movement of vehicles are considered.

This work is funded by the National Basic Research Program of China (No. 2006CB705500), the NNSFC under Project Nos. 10532060, 70601026, and 10672160, the CAS President Foundation, and by the China Postdoctoral Science Foundation (No. 20060390179). Y.-H. Wu acknowledges the support of the Australian Research Council through a Discovery Project Grant.

## References

1. K. Nagel, M. Schreckenberg, *J. Phys. I France* **2**, 2221 (1992)
2. D. Helbing, B.A. Huberman, *Nature (London)* **396**, 738 (1998)
3. B.S. Kerner, *The Physics of Traffic* (Springer, Berlin, New York, 2004)
4. D. Helbing, *Rev. Mod. Phys.* **73**, 1067 (2001)
5. T. Nagatani, *Rep. Prog. Phys.* **65**, 1331 (2002)

6. K. Nagel, P. Wagner, R. Woesler, *Oper. Res.* **51**, 681 (2003)
7. O. Biham, A.A. Middleton, D. Levine, *Phys. Rev. A* **46**, R6124 (1992)
8. D. Chowdhury, L. Santen, A. Schadschneider, *Phys. Rep.* **329**, 199 (2000)
9. A. Schadschneider, *Physica A* **313**, 153 (2002)
10. S. Maerivoet, B. De Moor, *Phys. Rep.* **419**, 1 (2005)
11. D.J. Watts, S.H. Strogatz, *Nature (London)* **393**, 440 (1998)
12. R. Albert, H. Jeong, A.L. Barabási, *Nature (London)* **401**, 130 (1999)
13. B. Jiang, C. Claramunt, *Environ. Plan. B: Plan. Des.* **31**, 151 (2004)
14. M. Rosvall, A. Trusina, P. Minnhagen, K. Sneppen, *Phys. Rev. Lett.* **94**, 028701 (2005)
15. P. Crucitti, V. Latora, S. Porta, *Phys. Rev. E* **73**, 036125 (2006)
16. P. Crucitti, V. Latora, S. Porta, *Chaos* **16**, 015113 (2006)
17. S. Porta, P. Crucitti, V. Latora, *Physica A* **369**, 853 (2006)
18. V. Kalapala, V. Sanwalani, A. Clauset, C. Moore, *Phys. Rev. E* **73**, 026130 (2006)
19. J. Sienkiewicz, J.A. Holyst, *Phys. Rev. E* **72**, 046127 (2005)
20. P. Li, X. Xiong, Z.L. Qiao et al., *Chin. Phys. Lett.* **23**, 384 (2006)
21. P. Sen, S. Dasgupta, A. Chatterjee et al., *Phys. Rev. E* **67**, 036106 (2003)
22. K.P. Li, Z.Y. Gao, B.H. Mao, *Inter. J. Mod. Phys. C* **17**, (2006) 1339
23. W. Li, X. Cai, *Phys. Rev. E* **69**, 046106 (2004)
24. Y. Moreno, R. Pastor-Satorras, A. Vazquez et al., *Europhys. Lett.* **62**, 292 (2003)
25. P. Echenique, J. Gómez-Gardeñes, Y. Moreno, *Europhys. Lett.* **71**, 325 (2005)
26. J.J. Wu, Z.Y. Gao, H.J. Sun et al., *Europhys. Lett.* **74**, 560 (2006)
27. M.B. Hu, W.X. Wang, R. Jiang et al., *Phys. Rev. E* **75**, 036102 (2007)
28. Z. Liu, M.B. Hu, R. Jiang et al., *Phys. Rev. E* **76**, 037101 (2007)
29. B. Hiller, J. Hanson J., *The Social Logic of Space* (Cambridge University Press, Cambridge, UK, 1984)
30. B. Hiller, *Space is the Machine: A Configurational Theory of Architecture* (Cambridge University Press, Cambridge, UK, 1996)
31. A. Penn, B. Hillier, D. Banister, J. Xu, *Environ. Plan. B* **25**, 59 (1998)
32. R.V. Sole, S. Valverde, *Physica A* **289**, 595 (2001)
33. A. Arenas, A. Díaz-Guilera, R. Guimerá, *Phys. Rev. Lett.* **86**, 3196 (2001)
34. B. Tadić, S. Thurner, G.J. Rodgers, *Phys. Rev. E* **69**, 036102 (2004)
35. L. Zhao, Y.C. Lai, K. Park, N. Ye, *Phys. Rev. E* **71**, 026125 (2005)
36. W.X. Wang, B.H. Wang, C.Y. Yin et al., *Phys. Rev. E* **73**, 026111 (2006)
37. R. Guimerá, A. Díaz-Guilera, F. Vega-Redondo et al., *Phys. Rev. Lett.* **89**, 248701 (2002)
38. J. Duch, A. Arenas, *Phys. Rev. Lett.* **96**, (2006) 218702; J. Duch, A. Arenas, *Eur. Phys. J. Special Topics* **143**, 253 (2007)